# Breakdown of invariant attractors for the dissipative standard map

Renato Calleja

Department of Mathematics

University of Texas at Austin

Austin TX, 78712 (USA)

(rcalleja@math.utexas.edu)

Alessandra Celletti

Dipartimento di Matematica

Università di Roma Tor Vergata

I-00133 Roma (Italy)

(celletti@mat.uniroma2.it)

July 9, 2009

**Abstract**

We implement different methods for the computation of the breakdown threshold of invariant attractors in the dissipative standard mapping. A first approach is based on the computation of the Sobolev norms of the function parametrizing the solution. Then we look for the approximating periodic orbits and we analyze their stability in order to compute the critical threshold at which an invariant attractor breaks down. We also determine the domain of convergence of the dissipative standard mapping by extending the computations to the complex parameter space as well as by investigating a two–frequency model.

# 1 Introduction

The existence of invariant attractors in nearly–integrable dissipative systems has been widely studied in the literature (see, e.g., [2], [7]). These attractors typically exist for specific values of the parameters. The existence domains in the parameter space, obtained through the analytical investigations, must be validated through numerical computations of the break–down threshold of the invariant attractor. In the present paper we develop several numerical techniques to provide reliable estimates of the critical values of the parameters

1

**at which the invariant attractor breaks–down. These methods are based on a suitable parametrization of the solution (which is found by a proper implementation of a Newton's method) and on the link of the invariant attractor with its approximating periodic orbits.**

As a specific model, we consider the dissipative standard map defined by the equations

$$
\begin{aligned}
y_{n+1} &= by_n + c + \varepsilon\, V'(x_n) \\
x_{n+1} &= x_n + y_{n+1}\ ,
\end{aligned}
\tag{1.1}
$$

where $y_n \in \mathbb{R}$, $x_n \in \mathbb{S}^1$, $b \in \mathbb{R}_+$, $c \in \mathbb{R}$, $\varepsilon \in \mathbb{R}_+$ and where $V = V(x)$ is an analytic, periodic function (the prime denotes derivative with respect to the argument). The mapping is ruled by two parameters: the *dissipative parameter* $b$ (which coincides with the determinant of the Jacobian associated to (1.1)) and the *perturbing parameter* $\varepsilon$. The quantity $c$ is called the *drift parameter*, which turns out to be equal to zero for $b = 1$. In this case one recovers the conservative mapping, which is integrable whenever the perturbing parameter is set to zero. We shall be interested in the cases $0 < b < 1$ and $\varepsilon > 0$. Unless explicitly stated, we shall be concerned with the choice $V(x) = -\frac{1}{(2\pi)^2} \cos(2\pi x)$, which recovers the classical standard mapping (see, e.g., [12], [13]).

In the conservative integrable case ($b = 1$, $\varepsilon = 0$), the standard map admits invariant curves with frequency $\omega$, provided $\omega$ satisfies the diophantine condition

$$
|\omega - \frac{p}{q}|^{-1} \le Cq^2\ , \qquad p, q \in \mathbb{Z}\ , \quad q \ne 0\ ,
$$

for some positive constant $C$. Here we will be concerned with two sample diophantine numbers[1], i.e. the golden ratio $\gamma_r = \frac{\sqrt{5}-1}{2} \simeq 0.6180$ and the noble irrational $\omega_1 = [0; 2, 5, 3, 1^\infty] \simeq 0.4567$. KAM theory ([15], [1], [22]) allows to state that an invariant curve with diophantine frequency $\omega$ persists under the perturbation, provided that the perturbing parameter $\varepsilon$ is sufficiently small. Computer–assisted applications of KAM theory allow to obtain refined lower bounds on the perturbing parameter, ensuring the existence of the invariant curve. In this context a number of numerical methods has been developed to evaluate the critical breakdown threshold of an invariant curve with diophantine frequency ([13], [16], [23]). In this work we address the same question in the dissipative setting ($0 < b < 1$) by looking for reliable techniques which allow to determine the breakdown threshold of invariant attractors (see, e.g., [3], [10], [11]). In particular, we investigate numerically the persistence of invariant attractors as the parameters $b$ and $\varepsilon$

---

[1]Using a continuous fraction representation the number $\omega \equiv [a_0; a_1, a_2, ...]$ with $a_j \in \mathbb{Z}$ corresponds to $\omega = a_0 + \frac{1}{a_1 + \frac{1}{a_2 + ...}}$; the symbol $1^\infty$ denotes an infinite sequence of ones.

are varied. We remark that a proof of the existence of invariant attractors (in a continuous model problem) has been given in [7] using a KAM approach (see also [2]).

The numerical computation of the breakdown threshold can be obtained through the analysis of the behavior of the parametric representation of the solution as $x = \vartheta + u(\vartheta)$, where $\vartheta \in \mathbb{S}^1$ and where $u = u(\vartheta)$ is a suitable periodic function; it is assumed that the variable $\vartheta$ varies linearly as $\vartheta_{n+1} = \vartheta_n + \omega$. Inserting the parametric representation in (1.1), one gets an equation for the function $u$ which can be solved through a Newton's method. The breakdown threshold of the invariant curve with frequency $\omega$ is obtained by computing suitable Sobolev's norms of the parametrizing function $u$ (see [5], [4], [6]). A validation of such result is given by the determination of the periodic orbits whose frequency is given by the rational approximants to the diophantine frequency of the invariant attractor. We remark that, as in the conservative case, the periodic orbits tend to the invariant attractor as the order of the approximation increases. We determine the stability threshold of such periodic approximants to infer the value of the breakdown threshold of the invariant attractor. The results are in full agreement with those obtained through the computation of the Sobolev's norms. We also determine the occurrence of the different attractors (either periodic or quasi–periodic) at the critical breakdown threshold for different values of the dissipative constant.

An analysis of the domain of existence of invariant attractors is performed using a complex value of the perturbing parameter; this study can be compared to results concerning the analyticity domain as computed, e.g., in [9]. We conclude with some remarks on the determination of the existence domain for a two–frequency model.

## 2   Newton's Method in 1-dimension

Quasi–periodic attractors associated to the dissipative standard map can be found using the parametric representation

$$x = \vartheta + u(\vartheta), \quad \vartheta \in \mathbb{S}^1 \ ,$$

where $u = u(\vartheta)$ is a periodic function. We assume that the variable $\vartheta$ varies linearly as $\vartheta_{n+1} = \vartheta_n + \omega$ ($n \in \mathbb{Z}_+$), where $\omega \in \mathbb{R} \setminus \mathbb{Q}$ is the rotation frequency. Looking for a quasi–periodic attractor amounts to solving the functional equation

$$E_c[u] \equiv u(\vartheta + \omega) - (1+b)u(\vartheta) + bu(\vartheta - \omega) - c - \varepsilon V'(\vartheta + u(\vartheta)) = 0 \ , \qquad (2.2)$$

where the unknowns are a smooth periodic function $u$ and a real number $c$. Once we find a pair $(u, c)$ satisfying (2.2), then the graph of the quasi–periodic attractor, invariant under

(1.1), is given by the parametrization

$$K(\vartheta) = \begin{pmatrix} \vartheta + u(\vartheta) \\ \omega + u(\vartheta) - u(\vartheta - \omega) \end{pmatrix} , \quad \vartheta \in \mathbb{S}^1 .$$

The solution $(u, c)$ of equation (2.2) will be found by means of the iteration of a Newton algorithm. More precisely, a Newton step consists in starting from a pair $(u_0, c_0)$ such that the norm of $E_{c_0}[u_0]$ is small; then one looks for a correction $(v, \delta)$ providing a new solution $(u_0 + v, c_0 + \delta)$ satisfying the functional equation

$$E_{c_0 + \delta}[u_0 + v] = 0$$

up to first order. In other words, $v$ must satisfy the linear equation

$$E'_{c_0}[u_0]v - \delta = -E_{c_0}[u_0] , \tag{2.3}$$

where the prime denotes the derivative with respect to the argument. As a consequence we obtain that the norm of $E_{c_0 + \delta}[u_0 + v]$ is of the order of the square of the norm of $E_{c_0}[u_0]$.

It is known from Nash–Moser theory ([25], [26]), that to set up a converging iterative Newton scheme it is not necessary to find an exact inverse of the operator $E'_{c_0}[u_0]$, but rather an approximate inverse will suffice to guarantee the convergence. Therefore, instead of finding $(v, \delta)$ from equation (2.3), we will rather use the relation

$$(v, \delta) = -\eta[u_0] E_{c_0}[u_0] ,$$

where $\eta[u_0]$ is an approximate inverse of $(E'_{c_0}[u_0], -1)$. In order to obtain such approximate inverse we use a modified version (see [24], [17]) of the Newton step provided by equation (2.3). In particular, we will find $(v, \delta)$ by solving the equation

$$h' E'_{c_0}[u_0]v - v E'_{c_0}[u_0]h' = -h'(E_{c_0}[u_0] - \delta) , \tag{2.4}$$

which is obtained from (2.3) by multiplying times $h' \equiv 1 + \frac{\partial u_0}{\partial \vartheta}$ and adding the extra term $-v E'_{c_0}[u_0]h'$. The advantage of the modified Newton step provided by equation (2.4) in comparison to the Newton step provided by equation (2.3) is that we are able to factorize the right hand side as a sequence of invertible operators, as shown in the following lemma.

**Remark 2.1** *We note that the modified version of the Newton step equation (see (2.4)) provides an advantage in terms of computational cost. The standard Newton's method (2.3) needs to invert a dense matrix (i.e. $E'_{c_0}[u_0]$) requiring $O(N^3)$ operations, if $N$ denotes the number of non–zero Fourier modes of the function $u_0$, while the modified version (2.4) requires only $O(N \log N)$ operations (compare with Algorithm 2.3 below).*

**Lemma 2.2** *Let us introduce the following definitions of the operators* $\Delta_{-1}$, $\Delta_1^b$:

$$
\begin{aligned}
\Delta_{-1}f(\vartheta) &\equiv f(\vartheta - \omega) - f(\vartheta) \\
\Delta_1^b f(\vartheta) &\equiv f(\vartheta + \omega) - bf(\vartheta) \ .
\end{aligned}
$$

*Then, assuming $E_{c_0}[u]$ as in (2.2), the modified Newton equation (2.4) is shown to be equivalent to the following equation:*

$$
\Delta_1^b[-h'(\vartheta)h'(\vartheta - \omega)\Delta_{-1}[(h')^{-1}v]] = -h'(E_{c_0}[u_0] - \delta). \tag{2.5}
$$

**Proof** . Assuming that the functions $v$ and $\delta$ satisfy (2.4), we compute the terms on the left hand side as follows:

$$
h'E_{c_0}'[u_0]v = h'(\vartheta)\{v(\vartheta + \omega) - (1 + b)v(\vartheta) + bv(\vartheta - \omega)\} - h'(\vartheta)\varepsilon V''(\vartheta + u_0(\vartheta))v(\vartheta)
$$

and

$$
vE_{c_0}'[u_0]h' = v(\vartheta)\{h'(\vartheta + \omega) - (1 + b)h'(\vartheta) + bh'(\vartheta - \omega)\} - v(\vartheta)\varepsilon V''(\vartheta + u_0(\vartheta))h'(\vartheta).
$$

Next we define $v(\vartheta) \equiv h'(\vartheta)w(\vartheta)$ and we use the definition of $\Delta_{-1}$ and $\Delta_1^b$ to get

$$
\begin{aligned}
h'E_{c_0}'[u_0]v - vE_{c_0}'[u_0]h' &= h'(\vartheta)h'(\vartheta + \omega)w(\vartheta + \omega) + bh'(\vartheta)h'(\vartheta - \omega)w(\vartheta - \omega) \\
&\quad - h'(\vartheta)h'(\vartheta + \omega)w(\vartheta) - bh'(\vartheta)h'(\vartheta - \omega)w(\vartheta) \\
&= \Delta_1^b[-h'(\vartheta)h'(\vartheta - \omega)(w(\vartheta - \omega) - w(\vartheta))] \\
&= \Delta_1^b[-h'(\vartheta)h'(\vartheta - \omega)\Delta_{-1}w(\vartheta)] \\
&= \Delta_1^b[-h'(\vartheta)h'(\vartheta - \omega)\Delta_{-1}[(h'(\vartheta))^{-1}v(\vartheta)]] \ ,
\end{aligned}
$$

which yields (2.5). $\square$

The Newton step consists in the following computational algorithm.

**Algorithm 2.3** *a) Find two functions $\varphi$ and $\nu$ solving the equations*

$$
\Delta_1^b \varphi = -h'E_{c_0}[u] \tag{2.6}
$$

*and*

$$
\Delta_1^b \nu = -h' \ . \tag{2.7}
$$

*Notice that if $\varphi$ and $\nu$ are solutions of (2.6) and (2.7), respectively, then for any $\delta \in \mathbb{R}$ the equation $\Delta_1^b(\varphi - \delta\nu) = -h'(E_{c_0}[u_0] - \delta)$ holds.*

b) *Choose $\delta \in \mathbb{R}$ such that*

$$\int_{\mathbb{T}} \frac{\varphi(\vartheta) - \delta\nu(\vartheta)}{h'(\vartheta)h'(\vartheta - \omega)} d\vartheta = 0 \ .$$

c) *Solve for $w$ from*

$$\Delta_{-1}w = \frac{\varphi - \delta\nu}{-h'(\vartheta)h'(\vartheta - \omega)} \ . \tag{2.8}$$

d) *Construct $v(\vartheta) = h'(\vartheta)w(\vartheta)$ and obtain the improved solution $(\tilde{u}, \tilde{c})$ defined as*

$$\tilde{u}(\vartheta) = u_0(\vartheta) + v(\vartheta) \ , \qquad \tilde{c} = c_0 + \delta \ .$$

The approximate inverse $\eta[u]$ is the operator obtained by performing the steps described in algorithm 2.3 and applying the inverse of $E_{c_0}[u_0]$ to $(v, \delta)$.

**Remark 2.4** *We note that all the above steps are diagonal either in Fourier space or in real space. More precisely, the steps in algorithm 2.3 can be accomplished by performing the following computations:*

- *arithmetic operations among functions and evaluation of some nonlinear functions;*

- *computation of derivatives of functions;*

- *finding the inverse of the operator $\Delta_1^b$, which is diagonal in Fourier space;*

- *finding the inverse of the operator $h'(\vartheta)h'(\vartheta - \omega)$, which is diagonal in real space;*

- *solving the following small divisor problem: find $w(\vartheta)$ solving (2.8) and such that*

$$\int_{\mathbb{T}} w(\vartheta) d\vartheta = 0 \ .$$

In order to implement numerically the Newton step described by the algorithm 2.3, it becomes natural to consider Fourier series of the form

$$u^{(N)}(\vartheta) = \sum_{|k| \leq N} \hat{u}_k \, e^{2\pi i k \vartheta} \ . \tag{2.9}$$

It is clear that we can store a function $u^{(N)}$ using either $N$ complex coefficients of the Fourier series or the values of $u^{(N)}$ on a grid of $N$ points in $\mathbb{C}$. Whenever the function $u^{(N)}$ is real, we will also have the following symmetry (the bar denotes complex conjugacy):

$$\hat{u}_k = \bar{\hat{u}}_{-k} \ .$$

6

Therefore, in the real case, we only need to store $\frac{N}{2} + 1$ coefficients. Notice that the cost of inverting the operators in Remark 2.4 is $O(N)$, since the operators are diagonal in real or Fourier space. Indeed, the most expensive operation in the Newton step 2.3 consists in passing from the real space to the Fourier Space. In our case, we have used FFT to accomplish this task, so that the cost of performing one Newton step is $O(N \log N)$ operations.

# 3 Breakdown threshold

In this section we aim to determine the breakdown threshold of quasi–periodic invariant attractors and to investigate related quantitative features.

## 3.1 Breakdown threshold through Sobolev's norms

The theoretical results described in [17], [5], [4] provide an algorithm for the computation of the analyticity breakdown; moreover such results allow to produce systematically a solution of the truncated equations. The rigorous results of [17], [5] show that if the approximate solution is well behaved, then there are true solutions in a neighborhood. It follows that, close to the breakdown, the smooth norms must blow up.

On the basis of this remark, we define the following norm. Let the Fourier expansion of a function $u = u(\vartheta)$ be written as $u = \sum_{k \in \mathbb{Z}} \hat{u}_k e^{ik\vartheta}$ and let $\|u\|_{L^2} \equiv \left( \sum_{k \in \mathbb{Z}} |\hat{u}_k|^2 \right)^{\frac{1}{2}}$. Then we define

$$\|u\|_r = \|\partial_\vartheta^r u\|_{L^2} + |\langle u \rangle| \ , \tag{3.10}$$

where $\partial_\vartheta^r$ denotes the $r$–th derivative with respect to $\vartheta$ and $\langle \cdot \rangle$ denotes the average with respect to $\vartheta$. Note that (3.10) is a norm on a space of periodic functions, which is in fact the only case we are interested in. For trigonometric polynomials as in (2.9) we consider the Sobolev norm defined as the following finite sum:

$$\|u^{(N)}\|_r = \left( \sum_{|k| \leq N} (2\pi k)^{2r} |\hat{u}_k|^2 \right)^{\frac{1}{2}} . \tag{3.11}$$

For numerical implementations we will be also interested in the norm of a partial tail defined within the range $\rho N \leq |k| \leq N$ for some $0 < \rho < 1$:

$$\|u^{(N)}\|_{r,\rho} = \left( \sum_{\rho N \leq |k| \leq N} (2\pi k)^{2r} |\hat{u}_k|^2 \right)^{\frac{1}{2}} .$$

Note that (3.11) makes sense even if $r$ is not an integer. Finally, the existence domain of invariant attractors can be computed using an approximate solution of (2.4) with $u_0$ represented by a trigonometric polynomial as in (2.9); a regular behavior of the Sobolev norm of $u^{(N)}$, as the parameters increase, provides evidence of the existence of the invariant attractor. The algorithm to identify the boundary of the existence domain can be described as follows.

**Algorithm 3.1**
*Choose a path in the parameter space starting with the integrable case.*
**Initialize**
    *$u^{(N)}$ for the integrable case*
**Repeat**
    *Increase the parameters along the path*
    *Run the Newton step (see Algorithm 2.3)*
    **If** *iterations of the Newton step do not converge*
        *decrease the increment in parameters*
    **Else** *(Iteration success)*
        *Record the values of the parameters*
        *and compute the Sobolev norm of the solution*
        **If** *the norm $\|u^{(N)}\|_{r,\rho}$ exceeds a threshold*
            *Double the number of Fourier coefficients and continue with $u^{(2N)}$*
**Until** *the Sobolev norm of the approximate solution exceeds a threshold*

Note that the arguments in [5] show that there will be an analytical solution in a neighborhood of the approximate solution, unless the Sobolev norm blows up. The simplest practical criterion for blow up is that the Sobolev norm reaches a threshold (in practical applications we select a threshold equal to $10^9$). A posteriori, one can check that the choice of the threshold does not affect much the final result. More accurate computations can be obtained by fitting the behavior of the norms at the blow up, a well established procedure in the conservative case.

Numerical evidence for the conservative case ($b = 1$) was found in [19], suggesting that invariant tori are regular at criticality. Therefore, since we are studying the blowup of the Sobolev norms, in practical computations we need to consider $r$ greater than 3. Different numerical algorithms were tested, since the Sobolev norm (3.10) is rather sensitive to round–off errors in the higher frequency terms. The breakdown of analyticity of the conservative standard map (i.e., the case $b = 1$) has been extensively studied, in particular using renormalization group techniques ([14], [20], [21]). These results show that if the

Sobolev norm of the function $u$, considered also as a function of $\varepsilon$ (say $u = u_\varepsilon$), blows up (in the conservative case), then it admits the asymptotic expression

$$||\partial_\vartheta^r u_\varepsilon||_{L^2} \approx \alpha|\varepsilon - \varepsilon_{crit}|^g \; , \tag{3.12}$$

where $\varepsilon_{crit}$ is the breakdown treshold, $\alpha$ is a scaling constant, and $g$ is the scaling exponent. Assuming the validity of (3.12), the values of $\varepsilon_{crit}$, $\alpha$ and $g$ can be estimated using a non linear regression.
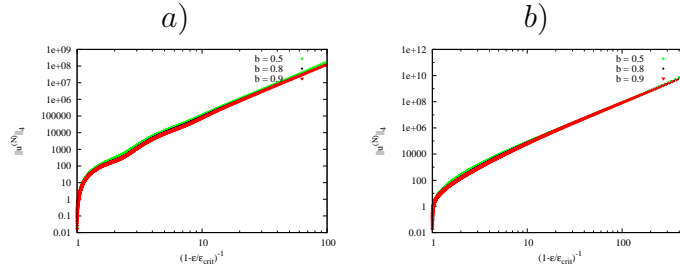


Figure 1: Norm $||u^{(N)}||_4$ plotted in logarithmic scale versus $\left(1 - \frac{\varepsilon}{\varepsilon_{crit}}\right)^{-1}$. $a$) Rotation number equal to $\omega_1 = [0; 2, 5, 3, 1^\infty]$. $b$) Rotation number equal to $\gamma_r$.

We implement the continuation algorithm 3.1 for the dissipative standard map and we plot the norm (3.10) for two different rotation numbers, namely $\omega_1 = [0; 2, 5, 3, 1^\infty]$ (see Figure 1$a$) and the golden ratio $\gamma_r = \frac{\sqrt{5}-1}{2}$ (see Figure 1$b$); the norm is displayed using logarithmic scale versus $\left(1 - \frac{\varepsilon}{\varepsilon_{crit}}\right)^{-1}$. In both figures we observe that $||u||_4$ tends asymptotically to a straight line. This allows to determine the scaling exponent $g$ introduced in (3.12) as the negative of the slope of the asymptotic line.

Table 1: Critical value $\varepsilon_{crit}$ and scaling exponent for three different values of $b$ and for the rotation numbers $\omega_1 = [0; 2, 5, 3, 1^\infty]$, $\gamma_r = \frac{\sqrt{5}-1}{2}$.

| $\omega_1$ | $b$ | $\varepsilon_{crit}$ | scaling exponent | $\gamma_r$ | $b$ | $\varepsilon_{crit}$ | scaling exponent |
|---|---|---|---|---|---|---|---|
| | 0.9 | 0.846356 | -3.10429 | | 0.9 | 0.972088 | -3.09997 |
| | 0.8 | 0.859174 | -3.06111 | | 0.8 | 0.973249 | -3.04985 |
| | 0.5 | 0.91968 | -3.14893 | | 0.5 | 0.979215 | -3.09517 |

Table 1 reports the values of $\varepsilon_{crit}$ for three different choices of $b$; it provides also the scaling exponent $g$, determined as the slope of the asymptotic lines, for the rotation frequencies $\omega_1$ and $\gamma_r$.

## 3.2 Approximation through periodic orbits

Using a well–known technique (see, for example, Greene's method presented in [13]) we determine the critical breakdown threshold of an invariant attractor by computing the sequence of periodic orbits approximating the frequency of the invariant attractor. Such periodic orbits are provided by the successive truncations of the continued fraction expansion of the frequency of the attractor. Indeed, for each set of values of the parameters there exists a whole interval of the drift parameter $c$ corresponding to a set of periodic orbits with fixed frequency (see [8]); in our computations it suffices to choose one of such periodic orbits. The periodic orbits with frequencies equal to the rational approximants to the frequency of the attractor converge to the invariant attractor as the order of the approximation increases (see Figure 2).
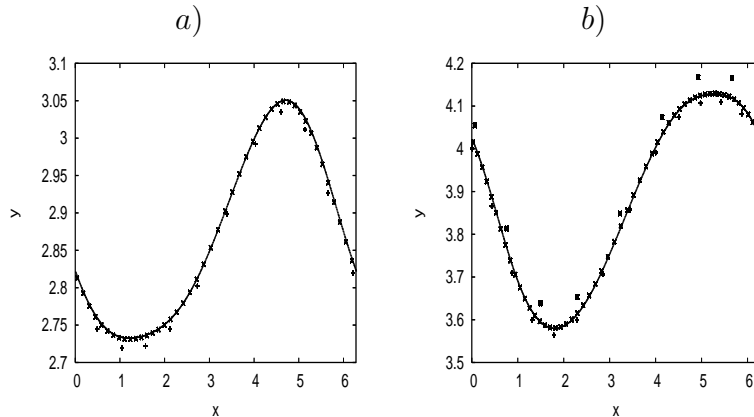


Figure 2: $a)$ For $b = 0.9$ and $\varepsilon = 0.3$ we display the graph of the invariant attractor with frequency $\omega_1$ and the periodic orbits with frequency $5/11$ $(+)$ and $21/46$ $(\times)$. $b)$ For $b = 0.9$ and $\varepsilon = 0.5$ we display the graph of the invariant attractor with frequency $\gamma_r$ and of the approximating periodic orbits with frequencies $5/8$ $(*)$, $8/13$ $(+)$, $34/55$ $(\times)$.

For the conservative standard map the breakdown of an invariant curve is strictly related to the stability character of the approximating periodic orbits. Let us denote the period by $p/q$ for some $p, q \in \mathbb{Z}$ with $q \neq 0$. In the dissipative case, for fixed values of the parameters there is a whole interval of the drift parameter $c$ which admits periodic orbits with period $p/q$. We select one of these trajectories and we evaluate its stability by computing the monodromy matrix associated to (1.1) along a full cycle of the periodic orbit. Let $T_{p,q}$ and $D_{p,q}$ be, respectively, the trace and the determinant of the monodromy matrix. In analogy to [13] we define the *residue* $R_{p,q}$ as the quantity

$$R_{p,q} \equiv \frac{1 + D_{p,q} - T_{p,q}}{2(1 + D_{p,q})} \ .$$

The eigenvalues $\lambda_{1,2}^{(p,q)}$ of the monodromy matrix are related to the residue by

$$\lambda_{1,2}^{(p,q)} = \frac{1}{2}(1 - 2R_{p,q})(1 + D_{p,q}) \pm \frac{1}{2}\sqrt{4R_{p,q}(R_{p,q} - 1)(1 + D_{p,q})^2 + (1 - D_{p,q})^2} \ .$$

Finally, the $p/q$–periodic orbit is stable if the residue belongs to the interval

$$R_-^{(p,q)} < R_{p,q} < R_+^{(p,q)} \ ,$$

where $R_\pm^{(p,q)} \equiv \frac{1}{2} \pm \frac{1}{2}\sqrt{1 - \frac{(1-D_{p,q})^2}{(1+D_{p,q})^2}}$. For a given value of the dissipative parameter $b$, we denote by $\varepsilon_{p,q}$ the maximal value of the perturbing parameter (assumed to vary in the interval $[0, 1)$) for which the periodic orbit with frequency $p/q$ is stable. Table 2 refers to $\omega_1$, while Table 3 refers to the golden ratio; in the latter case we selected the initial conditions as $(x_0, y_0) = (0, 2\pi\frac{p}{q})$, while in the first case we needed to be closer to the basin of attraction of the invariant curve by choosing $(x_0, y_0) = (0.0838, 2.0539)$. In both cases a preliminary set of $10^6$ iterations has been performed in order to get closer to the attractor; three sample values of the dissipative parameter $b$ have been considered. Both Tables show that the stability value seems to decrease toward a given threshold as the order of the periodic approximant is increased, thus defining a breakdown threshold of the invariant attractor. The results are consistent with those found in section 3.1.

Table 2: Stability threshold $\varepsilon_{p,q}$ of the periodic orbits approximating $\omega_1 = [0; 2, 5, 3, 1^\infty]$.

| $p/q$ | $\varepsilon_{p,q}(b = 0.9)$ | $\varepsilon_{p,q}(b = 0.8)$ | $\varepsilon_{p,q}(b = 0.5)$ |
|---|---|---|---|
| 5/11 | 0.816 | 0.814 | 0.919 |
| 16/35 | 0.877 | 0.877 | 0.952 |
| 21/46 | 0.865 | 0.876 | 0.939 |
| 37/81 | 0.861 | 0.872 | 0.929 |
| 58/127 | 0.853 | 0.866 | 0.927 |
| 95/208 | 0.848 | 0.863 | 0.922 |
| 153/335 | 0.847 | 0.863 | 0.920 |
| 248/543 | 0.847 | 0.861 | 0.920 |
| 401/878 | 0.847 | 0.864 | 0.919 |

## 3.3   Attractors at criticality

We evaluate the occurrence of the different attractors at criticality by implementing the following algorithm. Let us consider a given frequency $\omega$ (precisely, we shall take $\omega_1$ or

11

Table 3: Stability threshold $\varepsilon_{p,q}$ of the periodic orbits approximating $\gamma_r = \frac{\sqrt{5}-1}{2}$.

| $p/q$ | $\varepsilon_{p,q}(b=0.9)$ | $\varepsilon_{p,q}(b=0.8)$ | $\varepsilon_{p,q}(b=0.5)$ |
|---|---|---|---|
| 8/13 | 0.999 | 0.993 | 0.999 |
| 13/21 | 0.999 | 0.999 | 0.999 |
| 21/34 | 0.999 | 0.999 | 0.999 |
| 34/55 | 0.993 | 0.994 | 0.992 |
| 55/89 | 0.981 | 0.986 | 0.987 |
| 89/144 | 0.980 | 0.980 | 0.983 |
| 144/233 | 0.976 | 0.977 | 0.980 |
| 233/377 | 0.975 | 0.978 | 0.979 |
| 377/610 | 0.974 | 0.975 | 0.979 |

$\gamma_r$) and let us fix a specific value of the dissipative constant. Let $\varepsilon_{crit} = \varepsilon_{crit}(\omega)$ be the breakdown threshold of the invariant curve with frequency $\omega$, computed using the methods provided in sections 3.1, 3.2. For such critical perturbing parameter, we determine the value of the drift parameter $c$ corresponding to $\omega$. Next, we select $500 \times 500$ random initial conditions. For each initial condition, after a preliminary set of $10^6$ iterations, we determine the frequency of the different dynamical objects which attracted the trajectory starting from the given initial position. Tables 4 and 5 report the percentages of the occurrences of the different attractors for several values of the dissipative constant. We remark that for small values of $b$ the invariant attractor dominates, while for larger values of $b$ new periodic orbits appear as one gets closer to the conservative case.

Table 4: Occurrences of the attractors at criticality for different values of $b$ and for a value of $c$ associated to the invariant curve with frequency $\omega_1$.

| $b$ | $\varepsilon_{crit}$ | $\omega_1$ | 0/1 | 1/2 | 1/1 |
|---|---|---|---|---|---|
| 0.95 | 0.8410 | 35.43 % | 14.62 % | 36.42 % | 13.53 % |
| 0.9 | 0.8463 | 40.55 % | 11.84 % | 37.84 % | 9.77 % |
| 0.8 | 0.8590 | 53.46 % | 6.26 % | 37.15 % | 3.13 % |
| 0.7 | 0.8800 | 71.80 % | 0.08 % | 28.12 % | - |
| 0.6 | 0.8958 | 100 % | - | - | - |
| 0.5 | 0.9197 | 100 % | - | - | - |

Table 5: Occurrences of the attractors at criticality for different values of $b$ and for a value of $c$ associated to the invariant curve with frequency $\gamma_r$.

| $b$ | $\varepsilon_{crit}$ | $\gamma_r$ | 0/1 | 1/2 | 3/5 | 5/8 | 2/3 | 1/1 |
|------|--------|---------|---------|---------|--------|--------|--------|---------|
| 0.95 | 0.9624 | 31.35 % | 14.61 % | 20.47 % | 6.63 % | 0.42 % | 9.60 % | 16.92 % |
| 0.9 | 0.9747 | 52.46 % | 10.64 % | 15.55 % | - | - | 6.44 % | 14.91 % |
| 0.8 | 0.9732 | 89.96 % | 1.52 % | - | - | - | - | 8.52 % |
| 0.7 | 0.9751 | 94.14 % | - | - | - | - | - | 5.86 % |
| 0.6 | 0.9767 | 99.80 % | - | - | - | - | - | 0.20 % |
| 0.5 | 0.9807 | 100 % | - | - | - | - | - | - |

# 4  Existence domains for complex values of the perturbing parameter

We compute the solution of the functional equation (2.2) assuming that the perturbing parameter is complex, say $\varepsilon \in \mathbb{C}$. Applying Newton's method we follow the solution from $\varepsilon = 0$ increasing the real and imaginary parts. Let us write

$$\varepsilon = \varepsilon_r + i\varepsilon_i \ .$$

The expansion of the parametrization $u$ in terms of the complex $\varepsilon$ as the sum of a real and an imaginary part becomes

$$
\begin{aligned}
u(\vartheta; \varepsilon) &= \sum_{j=1}^{\infty} u_j(\vartheta)(\varepsilon_r + i\varepsilon_i)^j \\
&= u_r(\vartheta; \varepsilon_r, \varepsilon_i) + i u_i(\vartheta; \varepsilon_r, \varepsilon_i) \ ,
\end{aligned}
$$

where it is assumed that the functions $u_j(\vartheta)$ are real. Let us now turn to the expression for $V'(\vartheta + u(\vartheta))$; if we assume that $V'(\vartheta) = \frac{1}{2\pi k}\sin(2\pi k\vartheta)$, then we obtain the following expression:

$$
\begin{aligned}
V'(\vartheta + u_r + iu_i) &= -\frac{i}{4\pi k}[e^{-2\pi k u_i}(\cos(2\pi k(\vartheta + u_r)) + i\sin(2\pi k(\vartheta + u_r))) \\
&\quad - e^{2\pi k u_i}(\cos(2\pi k(\vartheta + u_r)) - i\sin(2\pi k(\vartheta + u_r)))] \ ,
\end{aligned}
$$

namely $V'(\vartheta + u_r + iu_i) = V'_r(\vartheta) + iV'_i(\vartheta)$, where

$$
\begin{aligned}
V'_r(\vartheta) &= \frac{1}{2\pi k}\cosh(2\pi k u_i)\sin(2\pi k(\vartheta + u_r)) \\
V'_i(\vartheta) &= \frac{1}{2\pi k}\sinh(2\pi k u_i)\cos(2\pi k(\vartheta + u_r)) \ .
\end{aligned}
$$

In particular, the product $\varepsilon V'(\vartheta + u)$ amounts to

$$\varepsilon V'(\vartheta + u) = \varepsilon_r V_r' - \varepsilon_i V_i' + i(\varepsilon_r V_i' + \varepsilon_i V_r') \ .$$

Setting $c = c_r + ic_i$, the functional equation (2.2) corresponds to the following two equations:

$$u_r(\vartheta + \omega; \varepsilon_r, \varepsilon_i) - (1 + b)u_r(\vartheta; \varepsilon_r, \varepsilon_i) + bu_r(\vartheta - \omega; \varepsilon_r, \varepsilon_i) - \varepsilon_r V_r'(\vartheta) + \varepsilon_i V_i'(\vartheta) - c_r = 0$$
$$u_i(\vartheta + \omega; \varepsilon_r, \varepsilon_i) - (1 + b)u_i(\vartheta; \varepsilon_r, \varepsilon_i) + bu_i(\vartheta - \omega; \varepsilon_r, \varepsilon_i) - \varepsilon_r V_i'(\vartheta) - \varepsilon_i V_r'(\vartheta) - c_i = 0 \ .$$

We report in Figure 3 the domains of existence in the complex $\varepsilon$–plane for different mappings, for the two frequencies considered in the previous sections and for some specific values of the dissipative constant. Looking at the shapes of the existence domains we observe a small loss of regularity as the dissipation increases. The cut of Figure 3c is possibly due to the fact that the frequency is close to a rational (compare with [9]). We also remark that the shapes of the existence domains strongly depend on the choice of the function $V'(\vartheta)$ (compare with Figure 3d).

# 5 Two parameters domain

We analyze the behavior of a mapping whose perturbing function contains two harmonics, each one multiplied by a different parameter, say $\varepsilon_1$ and $\varepsilon_2$:

$$V'(x) = \frac{\varepsilon_1}{2\pi} \sin(2\pi x) + \frac{\varepsilon_2}{4\pi} \sin(4\pi x) \ .$$

Following [4], [5], we compute the domain of existence of an invariant attractor with frequency $\omega$ by evaluating the breakdown threshold through the analysis of the Sobolev's norms as introduced in section 3.1. In particular we start from $\varepsilon_1 = \varepsilon_2 = 0$ and we use the continuation method along a straight line, until the Sobolev's norm of the parametrization exceeds a given value (typically $10^9$).

The results are presented in Figure 4, which shows that the area of the existence domain gets smaller as the system approaches the conservative limit; in particular, the folds disappear as we get closer to the circle–map case corresponding to $b = 0$. Indeed, we already stressed that the probability of finding an invariant attractor gets larger as the dissipative parameter $b$ decreases. We also remark that it was conjectured that the boundary of the existence domain is closely related to the stable manifold of the fixed point of the renormalization group transformation (see, e.g., [18]).
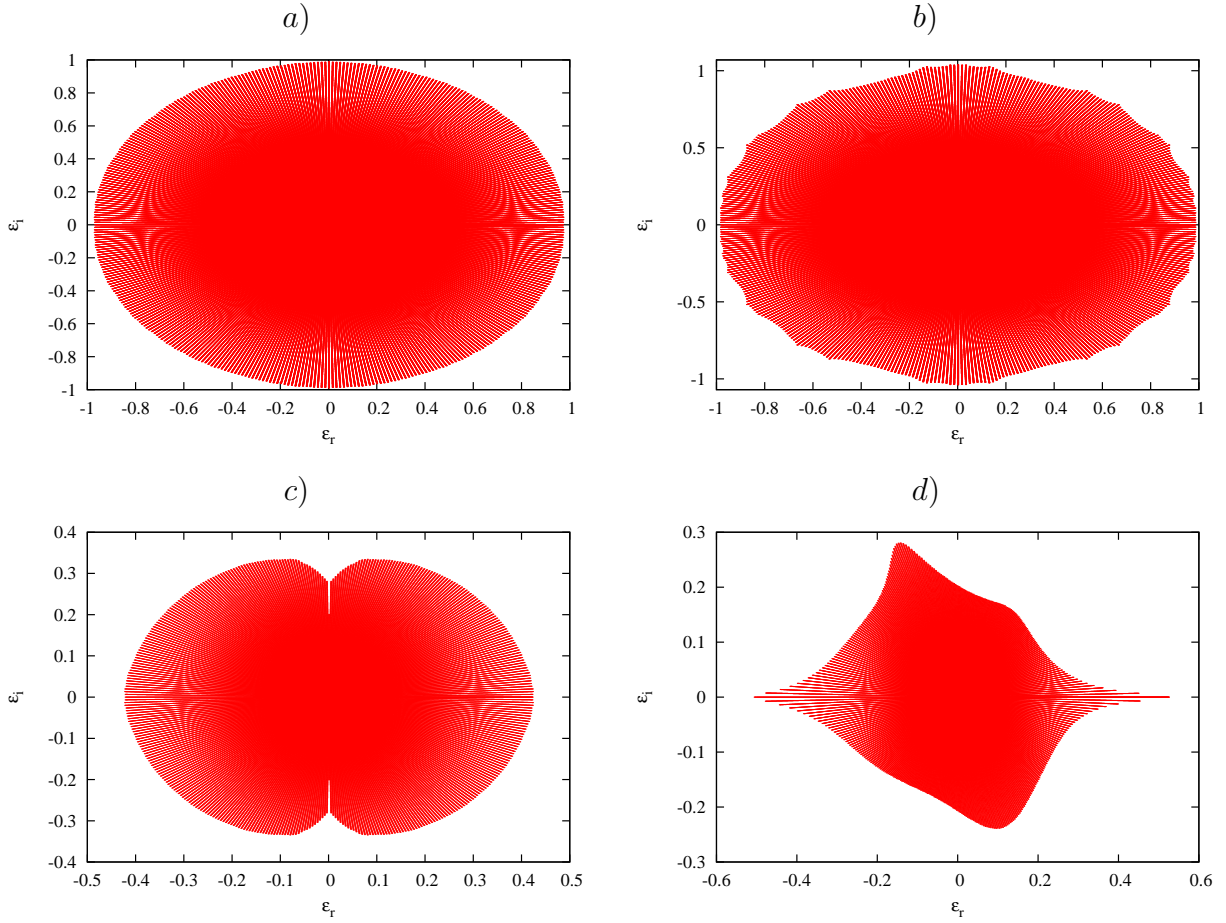
14

Figure 3: Existence domains for the dissipative standard map with complex perturbing parameter; the axes correspond to $\varepsilon_r$ and $\varepsilon_i$. a) $V'(x) = \frac{1}{2\pi}\sin(2\pi x)$, $\omega = \frac{\sqrt{5}-1}{2}$, $b = 0.9$; b) $V'(x) = \frac{1}{2\pi}\sin(2\pi x)$, $\omega = \frac{\sqrt{5}-1}{2}$, $b = 0.3$; c) $V'(x) = \frac{1}{2\pi}\sin(2\pi x)$, $\omega = [3, 12, 1, 1, 1, 1, ...]$, $b = 0.9$; d) $V'(x) = \frac{1}{2\pi}\left(\sin(2\pi x) + \frac{1}{20}\sin(4\pi x) + \frac{1}{30}\sin(6\pi x)\right)$, $\omega = \frac{\sqrt{5}-1}{2}$, $b = 0.9$.
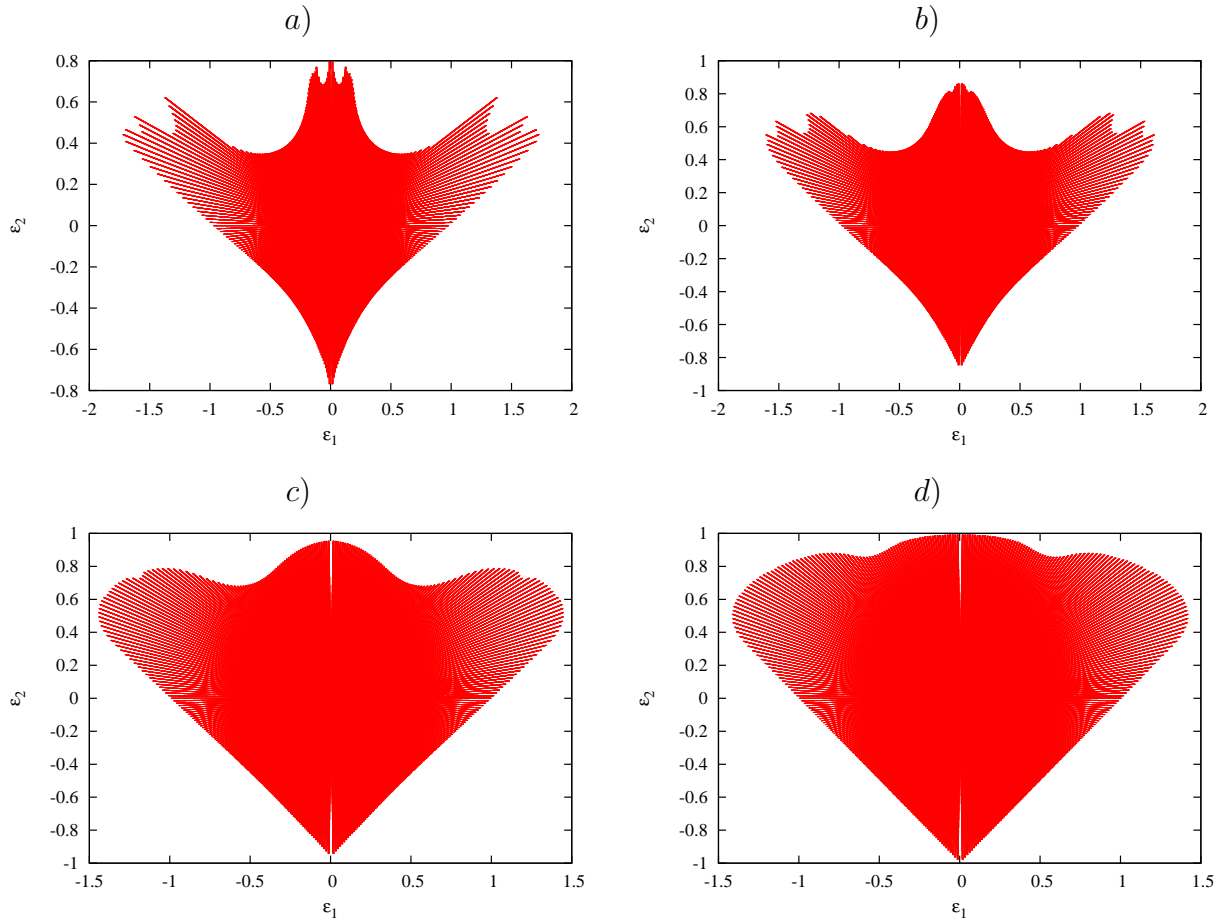
Figure 4: Existence domain for the two–frequency dissipative standard map in the parameter space $(\varepsilon_1, \varepsilon_2)$. The rotation number is equal to $\gamma_r = \frac{\sqrt{5}-1}{2}$. a) $b = 0.9$, b) $b = 0.5$, c) $b = 0.1$, d) $b = 0.01$.

16

# 6    Conclusions

Many important physical models are described as nearly–integrable systems subject to a dissipation. We can just mention, in solar system dynamics, the three–body problem with a Poynting–Robertson drag or the tidal torque due to the satellite's non–rigidity in the rotational dynamics. Invariant attractors are essential tools to explore the dynamics of this kind of models and a relevant issue is the computation of their break–down threshold, which is the subject of the present work.

This problem has been approached using a paradigmatic model, namely the dissipative standard map, which depends upon two parameters, namely the perturbing and the dissipative parameters. The results show that the break–down threshold can be effectively computed by determining a suitable parametrization of the invariant attractor, which is found by implementing a Newton's method. The computations are corroborated by a different technique, based on the determination of the stability property of the periodic orbits approximating the invariant attractor. Once the break–down threshold (in the perturbing parameter) has been determined, it was instructive to look for the attractors at criticality. It is found that periodic orbits are more frequent close to the integrable case, while invariant attractors dominate as the dissipative parameter gets smaller.

In the conservative setting a number of studies has been devoted to the determination of the domain of analyticity of the invariant curve for complex values of the perturbing parameter. In that case it was shown that the intersection of the boundary with the (positive) real axis provides a break–down threshold in agreement with that computed through Greene's method. Our study in the dissipative context shows that this remark applies also to the invariant attractors, since the intersection of the existence domain (see Figure 3a) with the real axis is in full agreement with the break–down threshold as provided by the Sobolev's norm criterion (see Table 3).

# References

[1] V.I. Arnold, *Small denominators and problems of stability of motion in classical and celestial mechanics*, Uspehi Mat. Nauk **18**, n. 6 (114), 91–192 (1963)

[2] H.W. Broer, G.B. Huitema, M.B. Sevryuk, *Quasi–periodic motions in families of dynamical systems. Order amidst chaos*, Lecture Notes in Mathematics **1645**, Springer–Verlag, Berlin (1996)

[3] H.W. Broer, C. Simó, J.C. Tatjer, *Towards global models near homoclinic tangencies of dissipative diffeomorphisms*, Nonlinearity **11**, 667–770 (1998)

[4] R. Calleja, *Existence and persistence of invariant objects in dynamical systems and mathematical physics*, The University of Texas at Austin, Ph.D. Thesis, 2009. Available at http://www.ma.utexas.edu/mp_arc-bin/mpa?yn=09-77

[5] R. Calleja, R. de la Llave, *Computation of the breakdown of analyticity in statistical mechanics models*, Preprint (2009), Available at http://www.ma.utexas.edu/mp_arc-bin/mpa?yn=09-56

[6] R. Calleja, R. de la Llave, *A criterion for the breakdown of quasi–periodic solutions and its rigorous justification*, Preprint (2009)

[7] A. Celletti, L. Chierchia, *Quasi–periodic attractors in Celestial Mechanics*, Archive for Rational Mechanics and Analysis **191**, 2, 311–345 (2009)

[8] A. Celletti, S. Di Ruzza, *Periodic and invariant attractors in a nearly–integrable dissipative mapping*, Preprint (2009)

[9] A. Celletti, C. Falcolini, *Singularities of periodic orbits near invariant curves*, Physica D **170**, n. 2, 87–102 (2002)

[10] A. Celletti, C. Froeschlé, E. Lega, *Dissipative and weakly–dissipative regimes in nearly–integrable mappings*, DCDS–A **16**, n. 4, 757–781 (2006)

[11] A. Celletti, R.S. MacKay, *Regions of non–existence of invariant tori for a spin–orbit model*, Chaos **17**, 043119, pp. 12 (2007)

[12] B.V. Chirikov, *A universal instability of many dimensional oscillator systems*, Physics Reports **52**, 264–379 (1979)

[13] J. Greene, *A method for determining the stochastic transition*, J. Math. Phys. **20**, 1183–1201 (1979)

[14] H. Koch, *A renormalization group fixed point associated with the breakup of golden invariant tori*, Discrete Contin. Dyn. Syst. **11**, 4, 881–909 (2004)

[15] A.N. Kolmogorov, *On the conservation of conditionally periodic motions under small perturbation of the Hamiltonian*, Dokl. Akad. Nauk SSSR **98**, 527–530 (1954)

[16] J. Laskar, C. Froeschlé, A. Celletti, *The measure of chaos by the numerical analysis of the fundamental frequencies. Application to the standard mapping*, Physica D **56**, 253–269 (1992)

[17] R. de la Llave, *KAM theory for equilibrium states in 1–D statistical mechanics models*, Annales Henri Poincarè **9**, 5, 835–880 (2008)

[18] R. de la Llave, A. Olvera, *The obstruction criterion for non–existence of invariant circles and renormalization*, Nonlinearity **19**, 1907–1937 (2006)

[19] R. de la Llave, N.P. Petrov, *Regularity of conjugacies between critical circle maps: an experimental study*, Experiment. Math. **11**, 2, 219–241 (2002)

[20] R.S. MacKay, *Renormalisation in area preserving maps*, PhD thesis, Princeton Univ. (1982)

[21] R.S. MacKay, *A renormalisation approach to invariant circles in area–preserving maps*, Physica D **7**, 1-3, 283–300 (1983)

[22] J. Moser, *On invariant curves of area–preserving mappings of an annulus*, Nach. Akad. Wiss. Göttingen, Math. Phys. Kl. II, 1 (1962)

[23] A. Olvera, C. Simó, *An obstruction method for the destruction of invariant curves*, Physica D **26**, 181–192 (1987)

[24] D.A. Salamon, E. Zehnder, *KAM theory in configuration space*, Comment. Math. Helv. **64**, 1, 84–132 (1989)

[25] E. Zehnder, *Generalized implicit function theorems with applications to some small divisor problems. I*, Comm. Pure Appl. Math. **28**, 91–140, 1975

[26] E. Zehnder, *Generalized implicit function theorems with applications to some small divisor problems. II*, Comm. Pure Appl. Math. **29**, 49–111, 1976